

Circulation Sensitivity to Tropopause Height

G. P. WILLIAMS

NOAA/Geophysical Fluid Dynamics Laboratory, Princeton University, Princeton, New Jersey

(Manuscript received 14 June 2005, in final form 24 January 2006)

ABSTRACT

The possibility that the tropopause could be lower during an ice-age cooling leads to an examination of the general sensitivity of global circulations to the tropopause height by altering a constant stratospheric temperature T_s in calculations with a dry, global, multilevel, spectral, primitive equation model subject to a simple Newtonian heating function. In general, lowering the tropopause by increasing the stratospheric temperature causes the jet stream to move to lower latitudes and the eddies to become smaller. Near the standard state with $T_s = 200$ K, the jets relocate themselves equatorward by 2° in latitude for every 5 K increase in the stratospheric temperature. A double-jet system, with centers at 30° and 60° latitude, occurs when the equatorial tropopause drops to 500 mb (for $T_s = 250$ K), with the high-latitude component extending throughout the stratosphere.

The eddy momentum flux mainly traverses poleward across the standard jet at 40° , in keeping with the predominantly equatorward propagation of the planetary waves. But when the jet lies at 30° (for $T_s = 225$ K) the flux converges on the jet in keeping with planetary waves that propagate both equatorward and poleward. Two sets of such wave propagation occur in the double-jet system. As the troposphere becomes even shallower, the flux reverts to being primarily poleward across the jet (for $T_s = 260$ K) but then becomes uniquely primarily equatorward across the jet (for $T_s = 275$ K) before the circulation approaches extinction. Thus the existence of a predominantly poleward flux in the standard state appears to be parametrically fortuitous.

1. Introduction

Studies with an aquaplanet model¹ of the atmospheric circulation that existed during the Last Glacial Maximum indicate that a cooling and shift in the sea surface temperature gradient may have led to a lower tropopause and to an equatorward shift in the westerly surface stress of up to 10° in latitude—see Williams and Bryan (2006) and the references therein. This raises questions as to how sensitive atmospheric circulations are in general to the height of the tropopause or to the thickness of the troposphere relative to the stratosphere.

This problem differs from the issue of determining

¹ Such a model has a realistic radiative heating, moist convection, and a simplified global ocean surface with preassigned surface temperatures.

Corresponding author address: Dr. G. P. Williams, NOAA/Geophysical Fluid Dynamics Laboratory, Princeton University, P.O. Box 308, Princeton, NJ 08542-0308.
E-mail: Gareth.Williams@noaa.gov

which tropospheric processes actually influence the formation of earth's tropopause, as discussed by Held (1982), Thuburn and Craig (2000), Haynes et al. (2001), and Schneider (2004). In the present study, the changes in tropopause height are enforced from above by altering the stratospheric temperature. Such states do not exist on earth to the extent developed but, like changes in the rotation rate, help define the range of atmospheric circulations for basic and planetary studies. The absence of moisture in our model also limits the applicability of the results but does not negate their basic nature.

The circulations are developed numerically using a dry, global, multilevel, spectral, primitive equation model subject to a simple Newtonian heating function that represents a linear relaxation to a specified temperature field. The relaxation temperature is set to a constant in the stratosphere and its value has a significant effect on the tropospheric circulation, primarily because it determines the location of the transition in the thermal equilibrium temperature profile. This constant is the only parameter varied in the present set of calculations. As we will see, lowering the tropopause

moves the jets from middle to low latitudes and thereby alters their character.

The behavior of earthlike jets lying in midlatitudes is well known: their eddy momentum flux is primarily poleward and due to neutral planetary waves propagating equatorward aloft after being generated by a baroclinic instability near the surface—see Held and Hoskins (1985) for a review of the process and theory. These characteristics alter, however, when the jets arise in lower latitudes. Such jets have more complex eddy fluxes and can easily be produced either by altering the rotation rate (Williams 1988) or by a heating that creates a baroclinic zone in lower latitudes (Williams 2003a,b). We now show that the circulation form can also vary for the standard baroclinicity and rotation rate when the height of the tropopause is altered.

The presentation begins in section 2 with a brief discussion of the numerical model and parameters. Section 3 then describes how the circulation changes when the stratospheric temperature is altered from 100 to 300 K in steps of 25 K, with 200 K being the standard value.

2. Numerical model

a. System of equations

The numerical model is based on the dynamical core of the Geophysical Fluid Dynamics Laboratory’s spectral GCM and is driven by a simple heating function, along the lines devised by Held and Suarez (1994). The primitive equations have the standard hydrostatic, vorticity–divergence form that is preferred for the semi-implicit, spectral transform scheme as summarized by Gordon and Stern (1982). The model predicts the zonal, meridional, and vertical velocity components (u , v , ω), plus the temperature and surface pressure fields (T , p_*), as a function of the latitude, longitude, and sigma coordinates (ϕ , λ , σ), where $\sigma = p/p_*$ is the normalized pressure. The variable $\psi(\phi, \sigma) = -\int \bar{v} \cos\phi d\sigma$ defines a quasi streamfunction for the zonally averaged meridional motion.

As well as a heating function, the equations include ∇^8 diffusion terms in the horizontal and, in the vertical, a linear boundary layer drag of the form

$$\frac{\partial(u, v)}{\partial t} \cdot \cdot \cdot = -k_V(\sigma)(u, v), \quad (1)$$

$$k_V = k_f \max\left(0, \frac{\sigma - \sigma_b}{1 - \sigma_b}\right), \quad (2)$$

where k_V^{-1} and σ_b define the time scale and the extent of the mixing. Topography, moisture, vertical diffusion, and convective adjustment are all omitted. The numeri-

cal procedure uses a triangular truncation at wavenumber 42 in the horizontal, with 30 equally spaced σ levels in the vertical.

b. Heating function

All flows are developed from an isothermal state of rest and are maintained by a Newtonian heating function of the form

$$\frac{\partial T}{\partial t} \cdot \cdot \cdot = -k_T(\phi, \sigma)[T - T_r(\phi, p)], \quad (3)$$

$$k_T = k_a + (k_s - k_a) \max\left(0, \frac{\sigma - \sigma_b}{1 - \sigma_b}\right) \cos^4\phi, \quad (4)$$

where the heating rate is proportional to the difference between the atmospheric temperature and a specified radiative relaxation temperature T_r . The relaxation damping rate $k_T(\phi, \sigma)$ is set to increase in the tropical boundary layer through the k_s factor to try to reduce the unrealistic cold layer that otherwise forms near the surface. The following distribution, as prescribed by Held and Suarez (1994),

$$T_r = \max\left\{T_s, \left[T_0 - (\Delta_H T) \sin^2\phi - (\Delta_V \Theta) \log\left(\frac{p}{p_0}\right) \cos^2\phi\right] \left(\frac{p}{p_0}\right)^\kappa\right\}, \quad (5)$$

provides the heating, where T_0 and T_s are tropospheric and stratospheric reference temperatures. The constants $\Delta_H T$ and $\Delta_V \Theta$ define the amplitude of the horizontal temperature and vertical potential temperature gradients.

c. Parameter values

The fixed physical parameters needed in the calculations use the following standard values: $a = 6370 \times 10^3$ m and $\Omega = 7.292 \times 10^{-5} \text{ s}^{-1}$ for the planetary radius and rotation rate; $g = 9.8 \text{ m s}^{-2}$ for the acceleration of gravity; $c_p = 1004 \text{ J kg}^{-1} \text{ K}^{-1}$ for the specific heat of air; $\kappa \equiv R/c_p = 2/7$, where R is the gas constant; $p_0 = 1000$ mb for a mean surface pressure based on the total mass p_0/g ; and $T_0 = 315 \text{ K}$ and $T_s = 100\text{--}300 \text{ K}$ (in steps of 25 K) for the reference temperatures. The other parameters are: $\sigma_b = 0.7$, $(k_f, k_a, k_s) = (1, 1/40, 1/4) \text{ day}^{-1}$, $\Delta_H T = 60 \text{ K}$, and $\Delta_V \Theta = 10 \text{ K}$.

In presenting the solutions, the figures use solid, dashed, and dotted contour lines to plot positive, negative, and zero values, respectively. The fields shown are time-averaged quantities, based on zonal means

sampled once a day over the last 300 days of 1000-day calculations.²

d. Analysis functions

The solutions are described using standard analysis procedures and notation, with the overbar and prime denoting the zonal mean and eddies. In particular, the Eliassen–Palm (EP) flux vector $\mathbf{F} = [F^{(\phi)}, F^{(p)}]$ and its scaling, together with the flux divergence E , are defined following Edmon et al. (1980) as

$$F^{(\phi)} = (-\overline{u'v'}) \frac{\cos^2 \phi}{a}, \quad (6)$$

$$F^{(p)} = \left(f \frac{\overline{v'\theta'}}{\overline{\theta}_p} \right) \cos^2 \phi, \quad (7)$$

$$E = \frac{\partial F^{(\phi)}}{\partial \phi} + \frac{\partial F^{(p)}}{\partial p}, \quad (8)$$

for the dominant geostrophic components, where $f = 2\Omega \sin \phi$.

3. The circulation set

a. Circulation range

We examine the sensitivity of the tropospheric circulation to the height of the tropopause as determined by a constant stratospheric temperature, T_s , which is altered from 100 to 300 K in steps of 25 K over nine cases. An extra case with $T_s = 260$ K is inserted into the sequence to examine the transition to extinction more closely. Normally, $T_s = 200$ K provides the standard (Held–Suarez) state.

In the solution set, the jet maximum moves from 55° to 15° in latitude and from σ equal 0.1 to 0.8 when the troposphere becomes shallower as T_s varies from 100 to 300 K, Fig. 1. The jet amplitude goes from 55 to 2 m s⁻¹, with the circulation approaching extinction when $T_s = 300$ K. However, at the other end of the range, below $T_s = 150$ K, the circulation hardly varies. The standard state lies in the most sensitive region where the jet relocates equatorward at a rate of 2° for every 5 K increase in T_s .³ Thus we concentrate on those cases lying between $T_s = 150$ K and 275 K, marked A–F in Fig. 1. The shallower circulations are less well resolved in the vertical and are more influenced by the boundary layer.

The primary fields are shown for the progressive

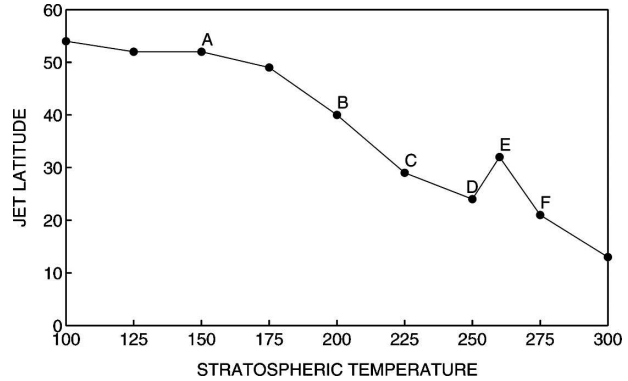


FIG. 1. Jet latitude as a function of the stratospheric temperature T_s . Cases A–F are presented in detail.

cases A–C in Fig. 2, and for the transitional and limiting cases D–F in Fig. 3, with each case occupying a single column. The thick curves superimposed on the temperature fields in Figs. 2b and 3b indicate the position of the radiative relaxation tropopause. All cases have eddy flux forms that are consistent with the theories describing nonlinear baroclinic instability and Rossby wave propagation. Consequently, we can rely on the EP cross sections to expose the processes underlying the eddy fluxes, Fig. 4.

b. Progressive circulations

The basic circulation, case B in Figs. 2a2–g2, has the well-known standard features for a dry idealized model: (a) a 35 m s⁻¹ jet at 40°, (b) Hadley and Ferrel cells with the same 27° width, (c) surface easterlies and westerlies coinciding with these two cells, (d) a poleward eddy heat flux, $\overline{v'T'}$, that extends over the hemisphere in the lower troposphere, with a secondary component at the tropopause, (e) a poleward eddy momentum flux, $\overline{u'v'}$, that coincides with the downward branch of the Hadley cell and the entire Ferrel cell and peaks near the tropopause, together with a weak equatorward component in high latitudes, (f) a $\overline{v'T'}$ cospectrum near the surface that peaks at zonal wavenumber $k = 6$ in the jet axis, and spreads to lower wavenumbers at higher latitudes, and (g) a $\overline{u'v'}$ cospectrum near the tropopause whose main component also peaks at $k = 6$ but in lower latitudes than the $\overline{v'T'}$ spectral peak, and whose weak equatorward component occurs at lower wavenumbers.

The B case also has the well-known standard EP features, Fig. 4b, namely, a flux divergence that accelerates the zonal wind near the surface and decelerates it aloft. The flux vector \mathbf{F} displays a wave propagation that is upward out of the baroclinic instability centered at 40°,

² Differences between the Northern and Southern Hemispheres provide a measure of the sampling limitations.

³ Such a T_s increase produces a 20-mb drop in the equatorial tropopause level.

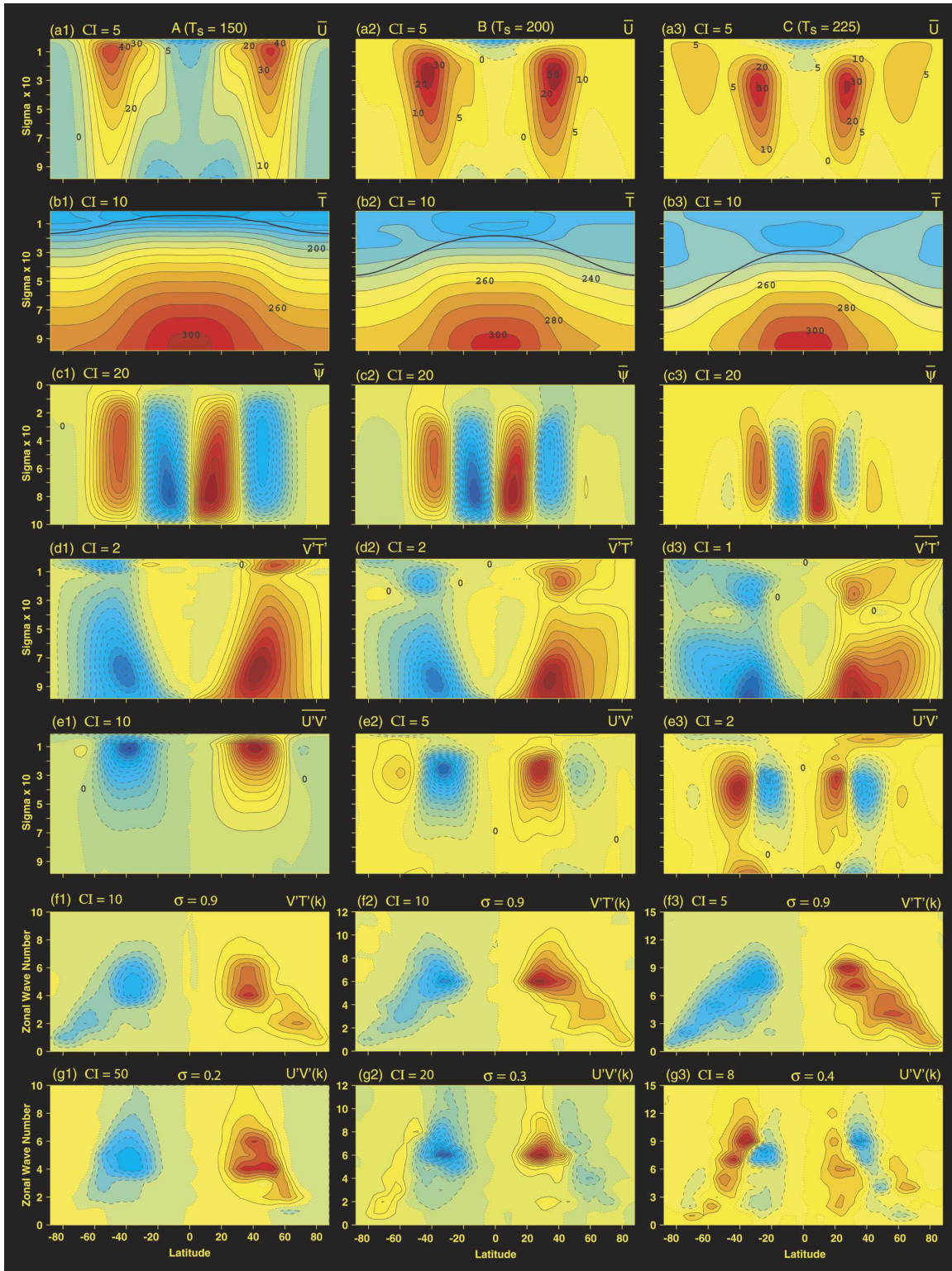


FIG. 2. Meridional sections of the primary mean, eddy, and spectral fields for the A–C solutions (one per column) with stratospheric temperatures T_s . Labels at the top of each panel indicate the field depicted, the contour interval (CI), and the σ level for the spectra. The contours have units: (a1)–(a3) m s^{-1} , (b1)–(b3) K, (c1)–(c3) s^{-1} , (d1)–(d3) K m s^{-1} , (e1)–(e3) $\text{m}^2 \text{s}^{-2}$, (f1)–(f3) K m s^{-1} , and (g1)–(g3) $\text{m}^2 \text{s}^{-2}$. The negative (zero) contours are dashed (dotted). The additional thick contour in the temperature fields indicates the position of the radiative relaxation tropopause.

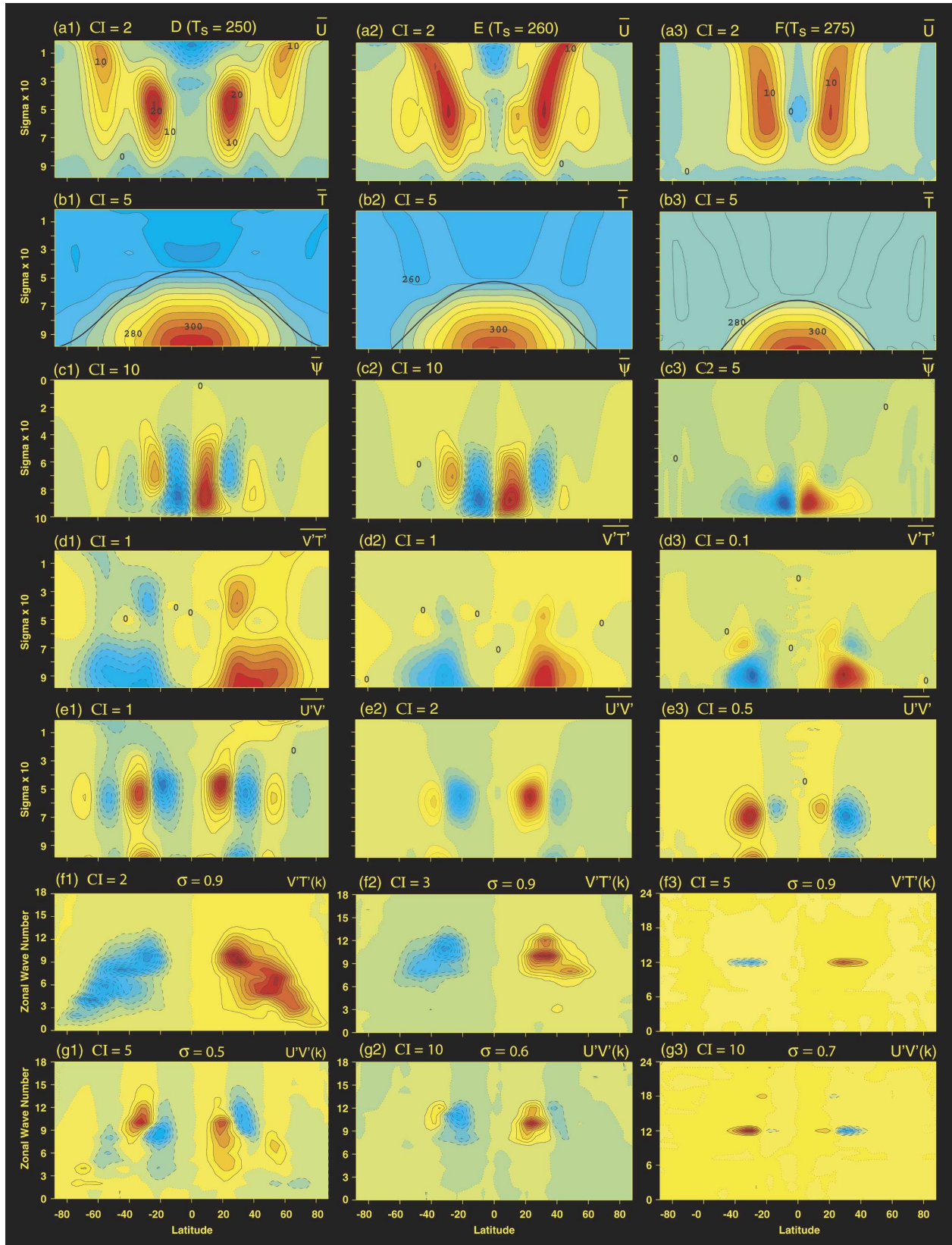


FIG. 3. Meridional sections of the primary mean, eddy, and spectral fields for the D-F solutions with stratospheric temperatures T_s . Notation and units as in Fig. 2.

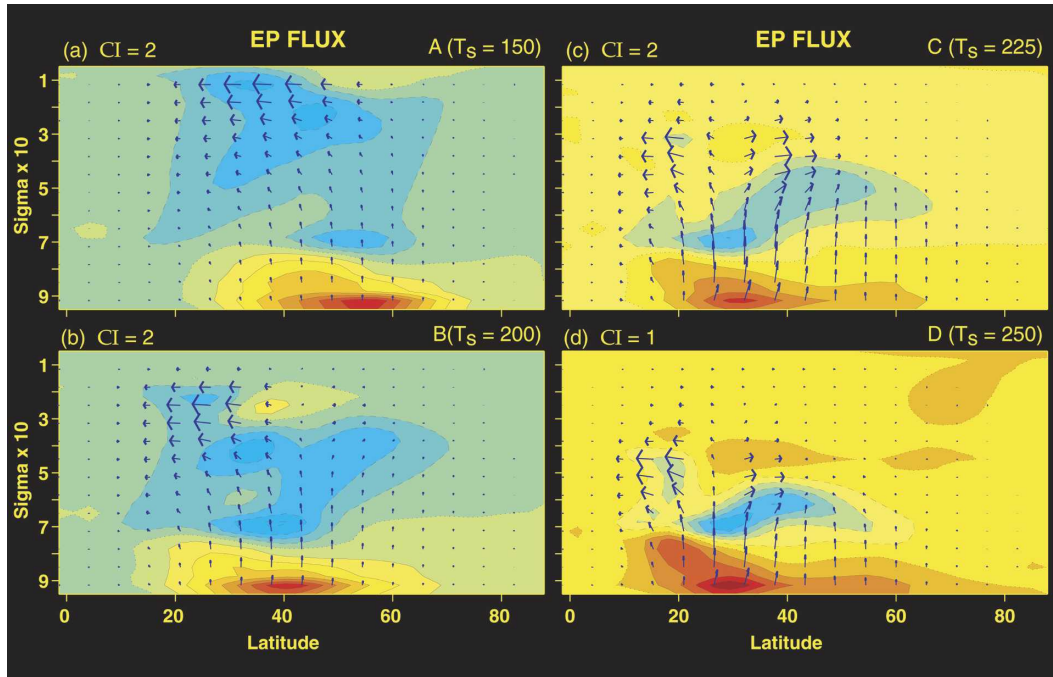


FIG. 4. Meridional sections of the Eliassen–Palm flux divergence E and flux vector \mathbf{F} for cases A–D with stratospheric temperatures T_s of (a)–(d) 150, 200, 225, and 250 K, respectively. The contour intervals (CI) are (a)–(c) 2, and (d) 1, in units of 10^{-5} m^2 . The negative (zero) contours are dashed (dotted).

then equatorward in Rossby waves near the tropopause, peaking at 30° before reaching extinction in critical layers extending over 5° – 10° .

When the tropopause is higher, as in case A with $T_s = 150 \text{ K}$ in Figs. 2a1–g1, the circulation has essentially the same form as the basic case. Except now the jet peaks at 52° and is wider, higher, and stronger (47 m s^{-1}), and is accompanied by 35° -wide cells and by eddies whose spectra peak at $k = 5$. The main qualitative difference occurs in the $\overline{u'v'}$ flux which is now entirely poleward. The EP scenario is very similar to case B, but with the instability centered at 55° and the Rossby waves peaking at 35° before expiring over 10° – 15° (Fig. 4a).

On the other hand, when the tropopause is lower, as in case C with $T_s = 225 \text{ K}$ in Figs. 2a3–g3, the jet peaks at 31 m s^{-1} in the subtropics near 29° and is accompanied by a weak (5 m s^{-1}) stratospheric jet in high latitudes. The Hadley and Ferrel cells are a narrower 20° in width, with the indirect cell becoming detached from the surface and a secondary direct cell arising in higher latitudes. The main change occurs in the $\overline{u'v'}$ flux in Fig. 2e3 which now has equal equatorward and poleward components, with the EP fields in Fig. 4c indicating that the Rossby waves generated by the baroclinic instability at 30° propagate both equatorward and poleward out of the jet axis. The equatorward $\overline{u'v'}$ component

also has a strong secondary contribution in the boundary layer.

The $\overline{u'v'}$ cospectrum in case C indicates that the upper-level Rossby waves generated by the instability propagate equatorward with a narrow peak at $k = 7$ but poleward with a broader peak over $k = 6$ – 9 . Neither set of waves propagates strongly into low or high latitudes. The $\overline{v'T'}$ cospectrum associated with the baroclinic instability is broader with a primary peak at $k = 9$ and a secondary peak at $k = 4$ in higher latitudes. Overall, the most energetic eddies are significantly smaller than in the standard case.

c. Transitional circulations

When the tropopause approaches the ground at the pole or in high latitudes, the baroclinic zone becomes subhemispheric in extent and the circulations undergo transitions, first to a double-jet state, then reverting to single jets with a different eddy character as the flows approach extinction, Fig. 3. Similar multijet states are also seen in high rotation systems (Williams 1988, 2003a; Lee 1997, 2005).

Such changes begin in case D (for $T_s = 250 \text{ K}$) where the main jet peaks at 22 m s^{-1} near 24° and where the second jet peaks at 12 m s^{-1} in high latitudes and extends throughout the troposphere and stratosphere. The jets are accompanied by four meridional cells in

each hemisphere, with the Hadley cell keeping a 20° width, but with the Ferrel cell becoming elevated and narrower as the eddies become smaller.

Likewise, the $\overline{u'v'}$ flux in case D has four components, with convergent zones near 25° and 60° , Fig. 3e1. For the related EP fields, in Fig. 4d, there are two pairs of equatorward plus poleward wave propagation, centered at these latitudes. They extend to 5° and 75° , respectively. The midlatitude poleward propagation and the weaker high-latitude equatorward propagation meet and stop at 46° ; the nature of their interaction, if any, is unknown. The $\overline{u'v'}$ cospectrum has two major components, with confined peaks at $k = 10$ for the poleward flux and at $k = 9$ for the equatorward flux. The secondary, high-latitude components occur at lower wavenumbers. The eddy heat flux, $\overline{v'T'}$, remains hemispheric but its spectrum becomes broader, with wave peaks at $k = 9, 6,$ and 4 .

A special case E with $T_s = 260$ K is added to the main set to examine the transition to the weak eddy state that occurs for $T_s = 275$ K. When the tropopause reaches the ground near 60° in case E, the two jets seen in case D appear to merge to form a strong zonal flow with a peak of 16 m s^{-1} and a highly tilted axis that extends throughout the troposphere and stratosphere, Fig. 3a2. As a result, the jet deviates from the tendency to move equatorward as the tropopause drops and lies more poleward than in cases C and D, Fig. 1. However, the Hadley cell keeps the same 20° width as seen in case C but is accompanied by a narrower Ferrel cell.

Also in case E, the $\overline{u'v'}$ flux reverts to the mainly poleward form seen in case B. The $\overline{v'T'}$ flux is no longer hemispheric, however, but remains confined to the baroclinic zone. Both spectra indicate that the eddies are limited to wavenumbers around $k = 10$ and have almost no activity at larger scales; in other words, the eddy activity becomes more limited again.

Finally, the limiting case F with $T_s = 275$ K marks the point at which the circulation approaches extinction (for the prescribed stratospheric formulation), Figs. 3a3–g3. The jet now peaks at 12 m s^{-1} near 21° and extends vertically throughout the troposphere and stratosphere, but with little axis tilt. The meridional circulation is unusual in that only a direct cell exists and appears to consist of two components, namely, a 20° -wide Hadley cell and a frictionally driven cell. The second component completely replaces the Ferrel cell below the $\sigma = 0.7$ level. The $\overline{u'v'}$ flux is also unusual in that the equatorward flux dominates, being a complete reversal of the standard state. Note, however, that all eddy fluxes are weak and mostly confined to the boundary layer. Both spectra are narrow, reflecting a flow that exhibits a steady wave form at $k = 12$.

4. Conclusions

By changing the value of one parameter, the stratospheric temperature T_s , which influences the height of the tropopause, it is possible to change the dynamical scales and the circulation forms in the model atmosphere. To begin with, we see a gradual progression in the single-jet circulation toward lower latitudes, with the Hadley and Ferrel cells becoming narrower until they reach a 20° limit, as T_s is varied from 150 to 225 K. This is followed by transitions to flows with: (a) a double jet and four cells at $T_s = 250$ K, (b) a strongly tilted low-latitude jet with narrow spectra at $T_s = 260$ K, (c) a deep jet with steady waves at $T_s = 275$ K, and (d) a weak (2 m s^{-1}) axisymmetric jet at $T_s = 300$ K (not shown), as the circulations approach extinction.

All of the flows presented are baroclinically unstable, with broader spectral peaks occurring when T_s lies in the 225–250-K range. The eddy momentum flux $\overline{u'v'}$ in the jets goes from being mainly poleward to convergent to mainly equatorward as the troposphere becomes shallower. The associated EP fields display a Rossby wave propagation aloft that goes from equatorward, to poleward plus equatorward, to poleward.

Most of the concepts of standard circulation theory seem to apply to the various solutions. For example, for a lower tropopause the eddies become smaller and the Ferrel cells narrower because their scale is primarily determined by the Rossby radius, $L_R = NH/f$, where N is the Brunt–Väisälä stability parameter, for a troposphere of thickness H . Furthermore, the jets move toward lower latitudes because the baroclinic zone shifts equatorward and the eddies become smaller when the tropopause is lower. The existence and width of the double jet (at $T_s = 250$ K) are consistent with the action of eddies at scales near the Rossby radius and the Rhines (1975) length, $L_\beta = (U/\beta)^{1/2}$, where U is the turbulence velocity amplitude. The double jets produced by a lower tropopause add another example of multiple jet formation to those usually brought about by higher rotation rates, as discussed recently by Lee (2005) and Williams (2003a).

There are two theoretical scales that may apply to the Hadley cell width. They are based on the hypotheses that an angular-momentum conserving flow extends poleward from the equator until either (a) the zonal flow matches the thermal wind, or (b) the vertical shear becomes baroclinically unstable. The first option gives an angular width $\theta_H \sim (R\Delta_H T)^{1/2}$, where $R = gH/(a\Omega)^2$, according to the axisymmetric theory of Held and Hou (1980). The Held–Hou scale appears to be more appropriate for the intense Hadley cells found in moist

models (Williams and Bryan 2006). On the other hand, the second option gives the traditional scale, $\theta_{BC} \sim (R\Delta_V T)^{1/4}$, a scale that seems to be the more appropriate for the present solutions as its value varies more slowly with changes in the tropopause height. However, neither theory really explains why the width of the Hadley cell never falls below 20° in the solutions.⁴

Concerning the existing atmospheric state, the form of the circulation appears to be relatively insensitive to the observed variations in the tropopause height. The solutions, however, indicate that a drop of about 100 mb (as when $T_s = 225$ K) could lead to Rossby waves propagating both poleward and equatorward from mid-latitudes, resulting in a change in the synoptic character of the circulation.

It should be emphasized that the circulations described by the solutions are not meant to represent observed or possible physical states but, rather, are designed to reveal trends and find alternative states by making extreme parameter changes. As such, they show that the standard jets relocate equatorward by 2° for every 5-K increase in the stratospheric temperature, as well as undergoing changes in the eddy character, primarily in the form of the eddy momentum flux and in the direction of the Rossby wave propagation. The presence of moist dynamical processes and interhemispheric differences would modify or complicate this behavior. Our dry model is too idealized to address issues of recent concern, such as changes in the tropopause height under increases in the greenhouse gases, changes in the location of the subtropical jet, or changes in the strength and width of the Hadley cell (Mitas and Clement 2005). However, the sensitivity of the Hadley cell and the annular mode to heating changes in moist models, as well as a comparison with data, are discussed in a related paper by Williams and Bryan (2006).

⁴ Additional calculations with an axisymmetric model are needed to define the low-tropopause states more fully, to determine in particular the extent to which the eddies influence the location and character of the various jets and cells.

Acknowledgments. I thank Kirk Bryan and Isaac Held for their interest in this study, and Catherine Raphael for organizing the graphics. I am also indebted to the reviewers for perceptive comments that substantially improved the presentation.

REFERENCES

- Edmon, H. J., B. J. Hoskins, and M. E. McIntyre, 1980: Eliassen-Palm cross sections for the troposphere. *J. Atmos. Sci.*, **37**, 2600–2616.
- Gordon, C. T., and W. F. Stern, 1982: A description of the GFDL global spectral model. *Mon. Wea. Rev.*, **110**, 625–644.
- Haynes, P., J. Scinocca, and M. Greenslade, 2001: Formation and maintenance of the extratropical tropopause by baroclinic eddies. *Geophys. Res. Lett.*, **28**, 4179–4182.
- Held, I. M., 1982: On the height of the tropopause and the static stability of the troposphere. *J. Atmos. Sci.*, **39**, 412–417.
- , and A. Y. Hou, 1980: Nonlinear axially symmetric circulations in a nearly inviscid atmosphere. *J. Atmos. Sci.*, **37**, 515–533.
- , and B. J. Hoskins, 1985: Large-scale eddies and the general circulation of the troposphere. *Advances in Geophysics*, Vol. 28A, Academic Press, 3–31.
- , and M. J. Suarez, 1994: A proposal for the intercomparison of dynamical cores of atmospheric general circulation models. *Bull. Amer. Meteor. Soc.*, **75**, 1825–1830.
- Lee, S., 1997: Maintenance of multiple jets in a baroclinic flow. *J. Atmos. Sci.*, **54**, 1726–1738.
- , 2005: Baroclinic multiple zonal jets on the sphere. *J. Atmos. Sci.*, **62**, 2484–2498.
- Mitas, C. M., and A. Clement, 2005: Has the Hadley cell been strengthening in recent decades? *Geophys. Res. Lett.*, **32**, L03809, doi:10.1029/2004GL021765.
- Rhines, P. B., 1975: Waves and turbulence on a beta plane. *J. Fluid Mech.*, **69**, 417–443.
- Schneider, T., 2004: The tropopause and the thermal stratification in the extratropics of a dry atmosphere. *J. Atmos. Sci.*, **61**, 1317–1340.
- Thuburn, J., and G. C. Craig, 2000: Stratospheric influence on tropopause height: The radiative constraint. *J. Atmos. Sci.*, **57**, 17–28.
- Williams, G. P., 1988: The dynamical range of global circulations—I. *Climate Dyn.*, **2**, 205–260.
- , 2003a: Jet sets. *J. Meteor. Soc. Japan*, **81**, 439–476.
- , 2003b: Barotropic instability and equatorial superrotation. *J. Atmos. Sci.*, **60**, 2136–2152.
- , and K. Bryan, 2006: Ice age winds: An aquaplanet model. *J. Climate*, **19**, 1706–1715.